DOI: 10.1002/cmdc.200600288

Virtual Screening Leads to the Discovery of an Effective Antagonist of Lymphocyte Function-Associated Antigen-1

Miyuki Shoda,[b] Takeo Harada,[b] Kazuo Yano,[b] Florence L. Stahura,[c] Takeshi Himeno,[b] Satoshi Shiojiri,[b] Yuji Kogami,[b] Hiroyuki Kouji,[b] and Jürgen Bajorath*[a]

The binding of lymphocyte function-associated antigen-1 (LFA-1) to its ligand on endothelial cells, intercellular adhesion molecule-1 (ICAM-1), is a crucial step in the migration of leukocytes during the early stages of inflammation and is also involved in T-cell activation. In this paper, we report the identification of a series of novel antagonists of the LFA-1/ICAM-1 interaction using ligand-based virtual screening (VS), analogue design, and structure–activity relationship (SAR) analysis. Candidate compounds were evaluated in protein binding and cell adhesion assays. Experimental evaluation of only 25 candidates selected from a pool of ~2.5 million database compounds identified an initial hit that could be expanded and converted into a lead that effectively blocked the interaction between LFA-1 and ICAM-1.

Introduction

LFA-1 is a member of the integrin family of cell surface proteins that are expressed on normal and also leukemia T cells.[1] The integrin LFA-1 consists of α-subunits (known as α_L or CD11a) and β-subunits (known as β_2 or CD18).[2] LFA-1 binds to intercellular adhesion molecules ICAM-1, -2, and -3 on the surface of different cell types and promotes a variety of homotypic and heterotypic cell adhesion events in the course of normal and also pathologic immune responses.[3] The LFA-1/ICAM-1 interaction plays a critical role in mediating cell adhesion, leukocyte transmigration, and augmentation of T-cell receptor signaling.[3] Small molecule antagonists of integrin–ligand interactions are thought to have significant therapeutic potential in the prevention of graft rejection after transplantation[4] and in the treatment of chronic inflammatory diseases such as psoriasis or rheumatoid arthritis.[5]

The α-subunit of LFA-1 contains a 200 amino acid domain known as the I-domain,[6] which is directly involved in the interaction with ICAM-1.[7] Several allosteric antagonists of LFA-1 function have been identified (Figure 1),[8] most of which bind to the I-domain (compounds **2** to **5** in Figure 1),[8] and the structural basis of their antagonistic effects has been explored.[9] Binding of diverse small molecule antagonists to a hydrophobic cleft within the I-domain prevents conformational changes that are essential for ICAM-1 binding and stabilizes the I-domain in its inactive conformation.[9–12] However, the currently most potent antagonist of the LFA-1/ICAM-1 interaction with a reported IC_{50} value of 1.4 nM for in vitro binding (compound **1** in Figure 1)[13] acts by another mechanism. Although it was originally designed to mimic the LFA-1 binding epitope of ICAM-1 by mapping side-chain functionality onto a small molecule template,[13] compound **1** and related active molecules[14,15] (also known as α/β I-like antagonists) do not bind to the ICAM-1 binding site in the I-domain but rather to a site at the interface between the α and β subunits of LFA-1. These compounds also function as allosteric antagonists,[13–15] albeit by a different mechanism than the known I-domain antagonists.

We set out to search compound databases for antagonists of the LFA-1/ICAM-1 interaction that are structurally distinct from those reported thus far. Although much has been learned about the structural foundations of LFA-1 antagonism, the spectrum of allosteric control of LFA-1 activation and interaction appears to be rather complex and structure-based design produced compounds that were active for reasons other than those expected.[13] Given this complexity, we have applied a ligand-based virtual screening approach using molecular similarity methods. These methods are based on a holistic molecu-

[a] *Prof. Dr. J. Bajorath*
Department of Life Science Informatics, B-IT,
Rheinische Friedrich-Wilhelms-Universität Bonn
Dahlmannstr. 2, 53113 Bonn (Germany)
Fax: (+49) 228-2699-341
E-mail: bajorath@bit.unibonn.de

[b] *M. Shoda, Dr. T. Harada, K. Yano, Dr. T. Himeno, S. Shiojiri, Y. Kogami, Dr. H. Kouji*
Laboratory For Drug Discovery, Research Center
Pharmaceutical R&D Division, Asahi KASEI Pharma Corporation,
632-1 Mifuku, Izunokuni-shi, Shizuoka (Japan)

[c] *Dr. F. L. Stahura*
Albany Molecular Research, Bothell Research Center,
18804 North Creek Parkway, Bothell, WA 98011-8012 (USA)

Supporting information for this article is available on the WWW under http://www.chemmedchem.org or from the author.

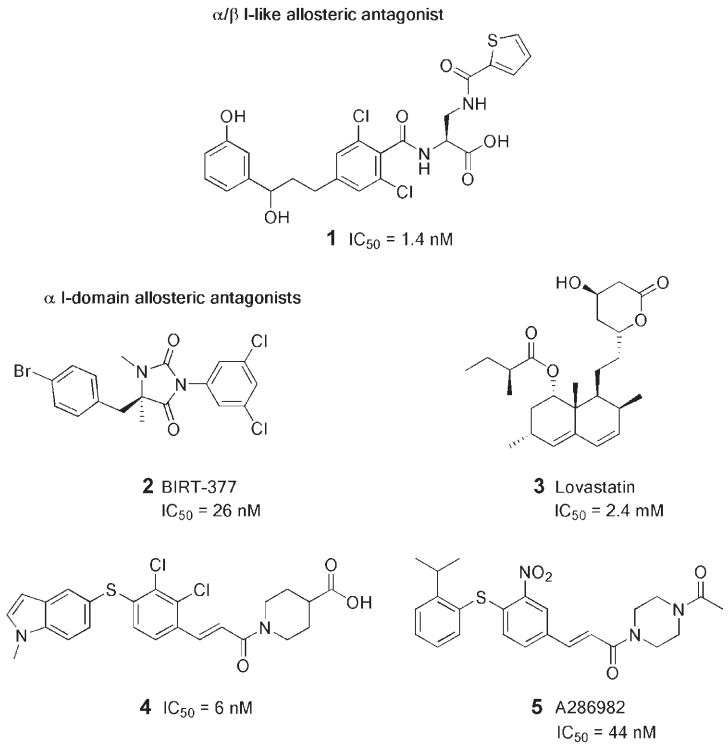

Figure 1. Structures of LFA-1/ICAM-1 antagonists. Compound **1**[13,14] was used as a single template for virtual screening. It targets a site in LFA-1 different from BIRT-377,[10] lovastatin,[9] compound **4**,[12] and antagonist A 286982.[11]

lar view and do not take structure-based design elements or pharmacophore information into account.[16] Our studies have led to the identification of a series of novel LFA-1 antagonists that were subjected to SAR analysis, leading to the generation of a lead compound that effectively blocked LFA-1 mediated cell adhesion.

Computational Methods

Using compound **1** as a template for virtual screening, we searched a compound database containing ~2.5 million virtually formatted compounds collected from catalogues of various chemistry vendors. For these calculations, a previously described small 2D fingerprint termed MFP (MiniFingerPrint) was used which consisted of fewer than 100 bits and combined value-range encoded property descriptors with binary structural fragment descriptors.[17] MFP belongs to a class of minifingerprints, a family of molecular fingerprints originally designed to recognize distant similarity relationships.[17] Database compounds were ranked according to their Tanimoto coefficient (Tc) values relative to compound **1**. Tc is defined as $b_{(ab)}/(b_{(a)}+b_{(b)}-b_{(ab)})$, with $b_{(a)}$ being the number of bits set on in fingerprint a, $b_{(b)}$ the number of bits set on in b, and $b_{(ab)}$ the number of bits shared by both fingerprints.[18] The top-ranked 50000 database compounds were preselected as a subset for further analysis. After addition of compound **1** as a "bait" molecule, the preselection set was subjected to cell-based partitioning calculations[19] using five different combinations of 1D/2D molecular descriptors that were previously found to perform well in classifying compounds having diverse biological activities.[19] Database compounds that fell into the same cells as compound **1** were selected as candidates.

Our intermediate selection set combined all database compounds that matched compound **1** with a Tc value greater than 0.8 and compounds that fell into cells containing compound **1** in at least two of five independent partitioning analyses using different descriptor sets. Each descriptor combination produces a different compound distribution and, therefore, recurrent copartitioning of database compounds with template compound **1** makes these molecules attractive candidates for further study. Intermediate compound selections were further analyzed using a scaffold analysis algorithm[20] to identify scaffold families or series of closely related analogues. This scaffold analysis algorithm removes substituents from ring systems of molecules, but does not break bonds between rings. Thus, it isolates ring-containing core structures. In addition, intermediate compound selections were filtered for rule-of-five compliance[21] and the presence of desired pharmacophore-like[22] and undesired reactive groups.[23] Database compounds passing these filters constituted our final VS selection set. Programs required for similarity searching, cell-based partitioning, and compound filtering were implemented in the Molecular Operating Environment (MOE).[24] Molecular descriptors were also calculated with MOE. After a novel hit was identified a hit expansion set was selected from the in-house compound database by substructure searching using a dehydro-amino acid amide as a query.

Results

We used compound **1** as a single template for MFP searching and arbitrarily preselected the top ranked 50000 compounds based on Tanimoto similarity to **1** for partitioning calculations.

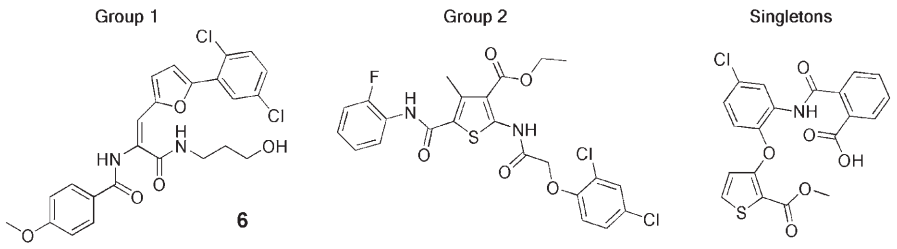

Figure 2. Compounds representative of the virtual screening selection set. Exemplary compounds representing scaffold families one and two are shown together with one of four singletons.

Candidate compounds were chosen if they mapped to the same cell as **1**, in at least two of five different partitioning calculations. This led to the selection of 19 candidate compounds. In addition, 27 compounds that matched template compound **1** with a Tc value above 0.8 were selected on the basis of fingerprint search calculations only. Seven candidate compounds were selected by both partitioning and fingerprint calculations. Thus, on the basis of our VS analysis, only 39 candidate compounds were selected from the source library containing ~2.5 million compounds. Moreover, only 25 of these 39 candidate molecules could be acquired for experimental evaluation. The test set contained molecules belonging to two scaffold families and four singletons. Representative compounds are shown in Figure 2 (and all compounds are provided in the Supplementary Information). Like the original selection, the reduced test set also contained molecules selected on the basis of similarity searching, partitioning, or both.

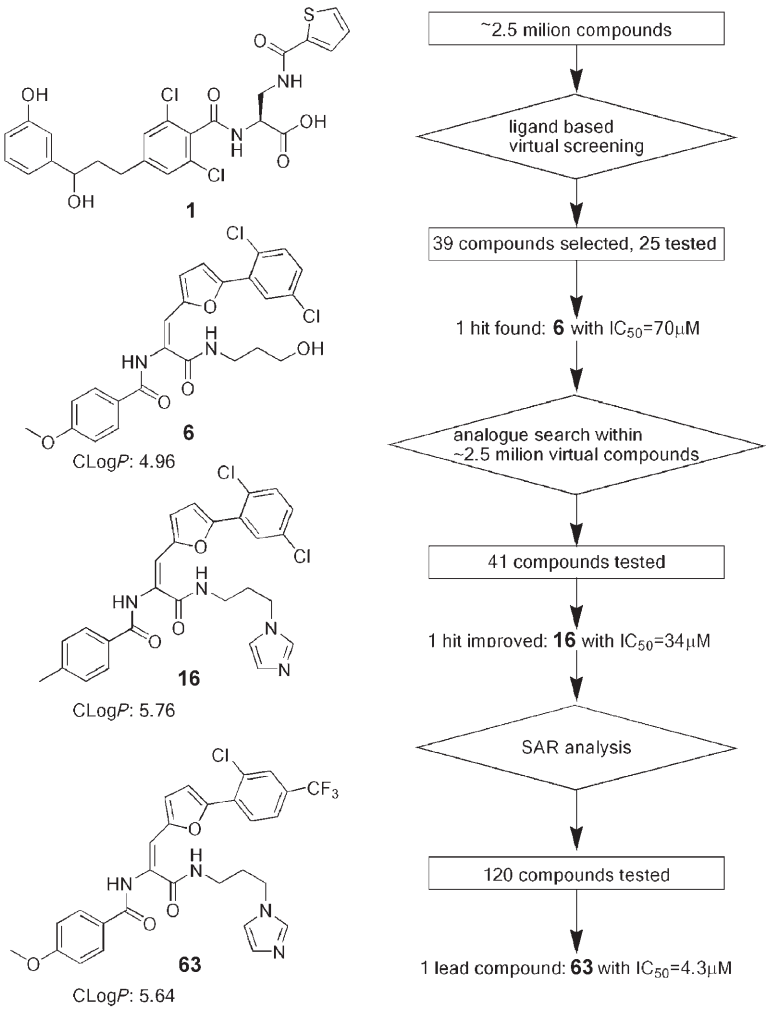

Figure 3. Summary of the strategy applied in the search for novel LFA-1/ICAM-1 antagonists.

Figure 3 summarizes the hit identification and expansion process. Among the selected compounds, **6** had a dehydro-alanine core structure and showed reproducible LFA-1/ICAM-1 antagonistic activity with an IC_{50} of 70 μM. Compound **6** belonged to scaffold group one in Figure 2. Other compounds in the test set sharing this scaffold did not show measurable activity (Table 1). Compound **6** was among the 27 molecules selected on the basis of fingerprint search calculations but was not found by partitioning analysis. Comparing compounds **1** and **6** using a fingerprint consisting of the set of 166 publicly available MACCS structural keys[27] gave a Tc value of 0.74 reflecting limited structural similarity.

Based on compound **6**, a dehydro-amino acid amide substructure search was carried out in an in-house compound database that identified 41 analogues of **6** for hit expansion. Out of those 41 compounds, seven compounds showed at least weak LFA-1/ICAM-1 antagonistic activity. Table 2 summarizes the results for all active and a subset of inactive analogues. Among these, compound **16** was most potent having an IC_{50} of 34 μM (Figure 3). The alternative stereoisomer of this compound was subsequently tested and found to be of comparable potency (Table 2). In three cases including compound **16**,

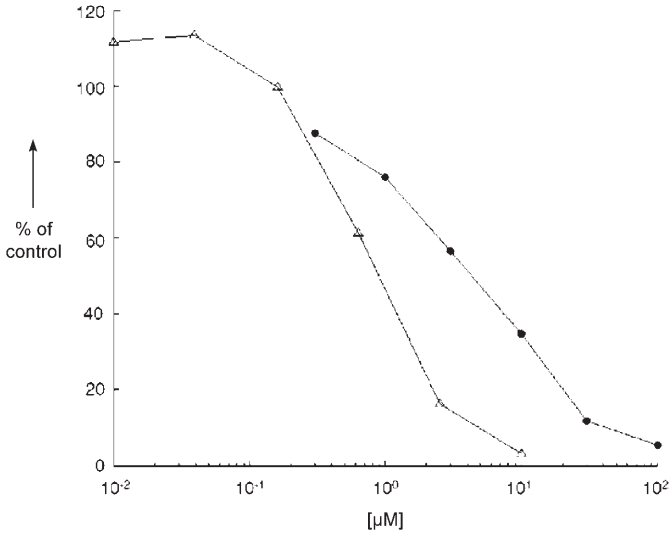

Figure 4. ELISA binding assay comparison of compound **63** and BIRT-377. "% of control" reports the antagonistic activity of **63** (black dots) in micromolar concentration relative to BIRT-377 (open triangles) as a positive control.

we found that stereoisomers had comparable potency. Thus, this series of antagonists was stereochemically permissive, suggesting that the stereocenter was not crucial for activity.

Assaying the hit expansion set revealed initial SAR data. We found that the combination of methoxy- or 4-toluoyl- groups at R^1, halogenated aryl-furanyl groups at R^2, and hydroxypropyl, imidazolylpropyl, or pyridylmethyl groups at R^3 were required for LFA-1/ICAM-1 antagonistic activity (Table 2).

On the basis of these observations, 120 dehydro-amino acid analogues were designed with combinations of methyl-, methoxy-, or halo-benzoyl groups at R^1, halogenated aryl-furanyl-groups at R^2, and alkyl-pyridyl-, alkyl-tertiary-amino-, or alkyl-imidazolyl-groups at R^3. Representative assay results for these series of analogues are reported in Table 3 and Table 4. Ten of these analogues displayed further increased potency with IC_{50} values <10 μM. CLog*P* values reported in Figure 1 revealed an unusually low value of compound **1** compared to other known antagonists that have CLog*P* values more comparable to those of our active compounds, as reported in Figure 3. Among the active analogues in Table 3 and Table 4, the most potent one was compound **63** displaying an IC_{50} value of 4.3 μM in the direct binding assay (Table 3, Table 4, and Figure 4). Compound **63** also had considerable activity in a Jurkat cell adhesion assay, with an IC_{50} value of 5.3 μM.

Discussion

Finding small molecule modulators or antagonists of protein–protein interactions continues to be a difficult task[8] and natural or induced allosteric regulatory sites in proteins[28] might often

Table 1. Antagonistic activity of dehydro-alanine derivatives.

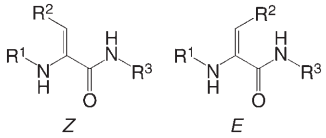

Compd	R^1	R^2	R^3	Stereoisomer	Binding[a]
6	4-methoxybenzoyl	5-(2,5-dichlorophenyl)-2-furanyl	3-hydroxypropyl	*E*	44.4
7	2-chlorobenzoyl	2-furanyl	3-carboxypropyl	*E*	101.1
8	2-chlorobenzoyl	2-furanyl	2-carboxyethyl	*E*	102.9
9	2-chlorobenzoyl	cinnamyl	2-carboxyethyl	*E*	108.7
10	2-furanoyl	4-chlorophenyl	2-carboxyethyl	*Z*	101.8
11	2-chlorobenzoyl	piperonyl	2-carboxyethyl	*Z*	94.8
12	2-bromobenzoyl	piperonyl	2-carboxyethyl	*Z*	103.2
13	4-bromobenzoyl	piperonyl	2-carboxyethyl	*E*	107.7
14	benzoyl	4-chlorophenyl	2-carboxyethyl	*Z*	103.0

[a] Binding refers to the LFA-1/ICAM-1 ELISA assay and the values given refer to % residual binding compared to wild type at 100 μM compound concentration.

Table 2. Potency of hit analogues with dehydro-amino acid amide core structure.

Compd.	R^1	R^2	R^3	Stereoisomer	Binding[a]
15	4-toluoyl	5-(2,5-dichlorophenyl)-2-furanyl	3-(1-imidazolyl)propyl	*Z*	34.3
16	4-toluoyl	5-(2,5-dichlorophenyl)-2-furanyl	3-(1-imidazolyl)propyl	*E*	30.5
17	4-methoxybenzoyl	5-(2,5-dichlorophenyl)-2-furanyl	3-(1-imidazolyl)propyl	*Z*	58.1
18	4-methoxybenzoyl	5-(2,5-dichlorophenyl)-2-furanyl	3-(1-imidazolyl)propyl	*E*	50.5
19	4-toluoyl	5-(4-bromophenyl)-2-furanyl	3-(1-imidazolyl)propyl	*E*	131.7
20	4-toluoyl	2-furanyl	3-(1-imidazolyl)propyl	*Z*	114.1
21	4-toluoyl	5-(3-nitrophenyl)-2-furanyl	3-(1-imidazolyl)propyl	*Z*	126.7
22	4-toluoyl	5-(2-nitrophenyl)-2-furanyl	3-(1-imidazolyl)propyl	*Z*	125.6
23	3,4-xyloyl	2-furanyl	3-(1-imidazolyl)propyl	*Z*	98.9
24	4-methoxybenzoyl	5-(3-trifluoromethylbenzoyl)-2-furanyl	3-(1-imidazolyl)propyl	*Z*	60.3
25	4-chlorobenzoyl	5-(3-trifluoromethylbenzoyl)-2-furanyl	3-(1-imidazolyl)propyl	*Z*	53.4
26	4-chlorobenzoyl	5-(4-chlorophenyl)-2-furanyl	3-(1-imidazolyl)propyl	*E*	83.7
27	4-methoxybenzoyl	5-(3,4-dichlorophenyl)-2-furanyl	3-(1-imidazolyl)propyl	*E*	67.5
28	benzoyl	5-(4-fluorophenyl)-2-furanyl	3-(1-imidazolyl)propyl	*Z*	123.6
29	benzoyl	2-furanyl	3-hydroxypropyl	*E*	98.0
30	4-toluoyl	5-(2,5-dichlorophenyl)-2-furanyl	cyclohexyl	*Z*	129.3
32	4-toluoyl	5-(2,5-dichlorophenyl)-2-furanyl	2-furanylmethyl	*Z*	121.4
33	4-toluoyl	5-(2,5-dichlorophenyl)-2-furanyl	benzyl	*Z*	86.0
34	4-toluoyl	5-(2,5-dichlorophenyl)-2-furanyl	2-methoxyethyl	*Z*	55.7
35	4-toluoyl	5-(2,5-dichlorophenyl)-2-furanyl	phenethyl	*Z*	94.9
36	4-toluoyl	5-(2,5-dichlorophenyl)-2-furanyl	methyl	*Z*	91.3
37	4-toluoyl	5-(2,5-dichlorophenyl)-2-furanyl	4-pyridylmethyl	*Z*	33.6
38	4-methoxybenzoyl	5-(3-chlorophenyl)-2-furanyl	3-(1-imidazolyl)propyl	*Z*	113.1
39	4-toluoyl	5-(2,4-dichlorophenyl)-2-furanyl	3-hydroxypropyl	*Z*	62.2

[a] Binding refers to the LFA-1/ICAM-1 ELISA assay and the values given refer to % residual binding compared to wild type at 100 μM compound concentration.

Table 3. Results of SAR analysis.[a]

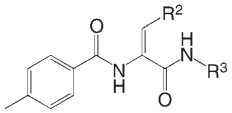

Compd	R^2	R^3	Binding assay IC_{50} [μM]	Cell adhesion block IC_{50} [μM]
40	5-(2-chloro-5-trifluoromethylphenyl)-2-furanyl	3-(1-imidazolyl)propyl	7.0	20.8
41	5-(2-chloro-5-trifluoromethylphenyl)-2-furanyl	4-pyridylmethyl	10.2	12.5
42	5-(2-chloro-5-trifluoromethylphenyl)-2-furanyl	3-pyridylmethyl	10.3	85.5
43	5-(2-chloro-5-trifluoromethylphenyl)-2-furanyl	2-(4-pyridyl)ethyl	19.8	>100
44	5-(2-chloro-5-trifluoromethylphenyl)-2-furanyl	3-(diethylamino)propyl	13.2	32.6
45	5-(2-chloro-5-trifluoromethylphenyl)-2-furanyl	2-(diethylamino)ethyl	12.4	33.4
46	5-(2-chloro-4-trifluoromethylphenyl)-2-furanyl	3-(1-imidazolyl)propyl	15.0	21.7
47	5-(2-chloro-4-trifluoromethylphenyl)-2-furanyl	4-pyridylmethyl	9.6	18.4
48	5-(2-chloro-4-trifluoromethylphenyl)-2-furanyl	3-pyridylmethyl	22.7	26.4
49	5-(2-chloro-4-trifluoromethylphenyl)-2-furanyl	2-(4-pyridyl)ethyl	16.9	13.6
50	5-(2-chloro-4-trifluoromethylphenyl)-2-furanyl	3-(diethylamino)propyl	14.5	19.2
51	5-(2-chloro-4-trifluoromethylphenyl)-2-furanyl	2-(diethylamino)ethyl	25.6	35.5
52	5-(2,4-dichlorophenyl)-2-furanyl	3-(1-imidazolyl)propyl	12.2	26.8
53	5-(2,4-dichlorophenyl)-2-furanyl	4-pyridylmethyl	18.0	19.2
54	5-(2,4-dichlorophenyl)-2-furanyl	3-pyridylmethyl	22.5	23.2
55	5-(2,4-dichlorophenyl)-2-furanyl	2-(4-pyridyl)ethyl	23.5	15.2
56	5-(2,4-dichlorophenyl)-2-furanyl	3-(diethylamino)propyl	22.0	39.5
57	5-(2,4-dichlorophenyl)-2-furanyl	5-(2,5-dichlorophenyl)-2-furanyl	>100	

[a] In Table 3 and 4, the potency of analogues was evaluated by determination of IC_{50} values for antagonism in the ELISA assay and for blocking cell adhesion.

present more promising targets for small molecule intervention than large and complex protein–protein interfaces.[8] From this point of view, LFA-1 presents a more suitable target for the inhibition or modulation of receptor–ligand interactions using small molecules than other single-path transmembrane immune cell surface receptors that lack allosteric control.

Herein, we have applied ligand-based VS techniques to search for LFA-1 antagonist candidates. Given the availability of I-domain antagonists and α/β I-like antagonists, we had to decide whether to base our in silico screening calculations on multiple reference compounds (I-domain antagonists) or a single (α/β I-like) antagonist. Combining these antagonists into one template set was not appropriate because they target different sites. Multiple reference compounds typically provide more information than single molecules and thus using I-domain antagonists as templates would have been a reasonable choice. However, we decided to use the only known α/β I-like LFA-1 antagonist (compound **1** in Figure 1) as a single template because we considered the interface between the α- and β- subunits of LFA-1 a particularly attractive target site. The high potency of compound **1** did not influence this decision because other LFA-1 antagonists were nearly as potent. Furthermore, VS hits are most often active in the micromolar range, if a transition from an optimized compound to an alternative active scaffold has successfully been made.[29]

It has been observed that small molecules binding to the same protein site can elicit their effects through different interactions[30] and even very similar structures might display differences in binding modes.[31] Through the choice of our template compound we indirectly targeted the α/β interface in LFA-1 but VS calculations did not take any additional protein structure, pharmacophore, or mechanistic information into account. In fact, the complications associated with the structure-based design and the prediction of binding interactions of compound **1**[13] could be considered as another reason to subject this molecule to global similarity analysis in the search for new active compounds.

From ~2.5 million database compounds, we selected a total of only 39 candidates on the basis of our computational analysis. Twenty five of these compounds could ultimately be acquired and tested, and among them was a hit structurally distinct from known LFA-1 antagonists. The initially identified antagonist belonged to a scaffold family for which multiple members were selected as candidates. Within this set, related analogues were found to be inactive, which emphasizes the importance of thorough analogue evaluation in VS[16] and compound library design.[32]

Substructure searching identified compound **16**, a slightly more potent analogue than our original hit **6**. The series was further advanced through SAR analysis that yielded lead compound **63** having an IC_{50} value of 4.3 μM in a direct binding assay and comparable potency in a cell adhesion assay. SAR analysis also revealed chemical requirements for LFA-1 binding. In our binding assay, the new lead compound was only approximately tenfold less potent than BIRT-377.

Table 4. Results of SAR analysis.

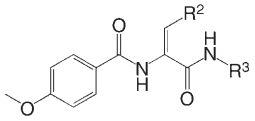

Compd	R^2	R^3	Binding assay IC_{50} [μM]	Cell adhesion block IC_{50} [μM]
58	5-(2-chloro-5-trifluoromethylphenyl)-2-furanyl	4-pyridylmethyl	16.3	22.0
59	5-(2-chloro-5-trifluoromethylphenyl)-2-furanyl	3-pyridylmethyl	8.2	12.4
60	5-(2-chloro-5-trifluoromethylphenyl)-2-furanyl	2-(4-pyridyl)ethyl	12.2	9.2
61	5-(2-chloro-5-trifluoromethylphenyl)-2-furanyl	3-(diethylamino)-propyl	14.5	49.3
62	5-(2-chloro-5-trifluoromethylphenyl)-2-furanyl	2-(diethylamino)ethyl	20.8	43.7
63	5-(2-chloro-4-trifluoromethylphenyl)-2-furanyl	3-(1-imidazolyl)propyl	**4.3**	**5.3**
64	5-(2-chloro-4-trifluoromethylphenyl)-2-furanyl	4-pyridylmethyl	8.5	10.1
65	5-(2-chloro-4-trifluoromethylphenyl)-2-furanyl	3-pyridylmethyl	14.0	>100
66	5-(2-chloro-4-trifluoromethylphenyl)-2-furanyl	2-(4-pyridyl)ethyl	10.9	9.2
67	5-(2-chloro-4-trifluoromethylphenyl)-2-furanyl	3-(diethylamino)-propyl	4.3	37.0
68	5-(2-chloro-4-trifluoromethylphenyl)-2-furanyl	2-(diethylamino)ethyl	9.4	28.5
69	5-(2,4-dichlorophenyl)-2-furanyl	3-(1-imidazolyl)propyl	6.7	20.4
70	5-(2,4-dichlorophenyl)-2-furanyl	4-pyridylmethyl	8.8	19.9
71	5-(2,4-dichlorophenyl)-2-furanyl	3-pyridylmethyl	13.8	30.4
72	5-(2,4-dichlorophenyl)-2-furanyl	2-(4-pyridyl)ethyl	5.3	42.0
73	5-(2,4-dichlorophenyl)-2-furanyl	2-(diethylamino)ethyl	14.3	39.7

Conclusions

Through a combination of virtual compound screening, analogue design, and SAR analysis, we have identified a novel antagonist of the LFA-1/ICAM-1 protein–protein interaction that has considerable potency. The initial hit was identified by testing of only 25 compounds taken from a large library containing ~2.5 million molecules. These findings illustrate the potential of VS to aid in the identification of novel active molecules.

Experimental Section

Compounds tested during the first and second stage were purchased from various vendors and those tested during the third stage were custom-synthesized on the basis of our SAR consideration by ASINEX (Moscow, Russia). Candidate compounds from virtual screening were evaluated using a competitive ELISA binding assay and a cell-based adhesion assay. For ELISA assays, Maxisorb (Nunc) 96-well immunoplates were used. ICAM12Fc, a chimeric protein consisting of human ICAM-1 domains one and two fused to the Fc region of human IgG1, and recombinant LFA-1 were prepared as described previously.[25] A goat-antihuman IgG Fc antibody and horse radish peroxidase (HRP) conjugated anti-LFA-1 monoclonal antibody (HB244 mAb, directed against the LFA-1 alpha subunit), were obtained from the American Type Culture Collection. For the LFA-1/ICAM-1 binding assay, 50 μL of antihuman-Fc antibody (5 $\mu g\,mL^{-1}$) in HBS buffer (0.15 M NaCl/10 mM HEPES, pH 7.4) were used to coat wells of 96-well microtiter plates overnight at 4 °C. The wells were then washed five times with assay buffer (AB: 2 mM $MgSO_4$/2 mM $CaCl_2$/HBS) and incubated with 50 μL of ICAM-Fc (2 $\mu g\,mL^{-1}$)/1% BSA/AB) overnight at 4 °C. After washing with AB, serial dilutions of compounds and purified LFA-1 in 1% BSA/AB (total volume 50 μL) were incubated for 4 h at 25 °C to test for antagonistic activity. After washing with AB, 50 μL of antiLFA-1 mAb-HRP conjugate (0.5 $\mu g\,mL^{-1}$) were added to the wells to detect bound LFA-1. Incubation proceeded for 2 h at 25 °C. The wells were washed and 100 μL thymolphthalein monophosphate (TMB) were added. After incubation for 20 min at room temperature, 100 μL of 2 N H_2SO_4 was added and absorbance at 450 nm (A450) was measured. The percent inhibition of each compound was calculated using the following equation:

% inhibition = 100((1−(A450 with compound minus background)/(A450 without compound minus background)), where background was A450 in the presence of 25 mM EDTA which inhibited binding of LFA-1 to ICAM-Fc.

The ICAM-1/Jurkat cell adhesion assay was carried out according to Rothlein et al.,[26] with some modifications. For measurement of antagonistic activity in the cell-based adhesion assay, 96-well microtiter plates were coated with 50 μL of human ICAM-Fc fusion protein at a concentration of 10 $\mu g\,mL^{-1}$ in HBS overnight at 4 °C. The wells were then washed twice with HBS and blocked by addition of 50 μL of 1% BSA/HBS by incubation for 2 h at 25 °C. Jurkat cells were suspended in BGH (0.1% BSA/2 $mg\,mL^{-1}$ glucose/HBS) and added to the wells (20×10^4 cells/well). Serial dilutions of test compounds were also added to the wells. The cells were stimulated by 0.5 mM $MgSO_4$. Microtiter plates were incubated for 1 h at 37 °C. After addition of 50 μL of 50% percoll/HBS, the wells were gently shaken and washed twice with 200 μL of HBS. Cells adhering to the wells were measured by acid phosphatase activity of the cells. Assay buffer (200 μL of 6 $mg\,mL^{-1}$ 4-nitrophenyl phosphate/1% Triton X-100/50 mM sodium acetate (pH 5.0)) was added to the wells and incubated for 5 min with shaking at room temperature. To stop the reaction, 50 μL of 5 N NaOH were added. The difference of the absorbance between 405 nm and 650 nm (A405–A650) was measured. The percent inhibition of each compound at each given concentration was calculated using the following equation:

% inhibition = 100((1−(A405–A650) with compound minus background)/((A405–A650) without compound minus background)) where background was (A405–A650) with nonstimulated Jurkat cells.

Supporting Information. Molecular descriptors used for compound partitioning are reported in Supporting Information Table 1 and candidate compounds selected from virtual screening calculations are provided in Supporting Information Figure 1.

Acknowledgement

The authors thank the following colleagues for their support of the project and their help in the characterization of compounds, Yurika Nagumo, Mayumi Shiozaki, Mizuka Tagashira, Shino Bito, and Toshiyuki Kodama. We particularly thank Setsuko Yamaguchi for skillful technical assistance with the biological assays.

Keywords: biological activity · cell adhesion antagonists · drug discovery · structure–activity relationships · virtual screening

[1] E. Martz, *Hum. Immunol.* **1987**, *18*, 3 – 37.
[2] C. G. Gahmberg, *Curr. Opin. Cell Biol.* **1997**, *9*, 643 – 650.
[3] S. D. Marlin, T. A. Springer, *Cell* **1987**, *51*, 813 – 819.
[4] E. K. Nakakura, R. A. Shorthouse, B. Zheng, S. M. McCabe, P. M. Jardieu, R. E. Morris, *Transplantation* **1996**, *62*, 547 – 552.
[5] K. Yonekawa, J. M. Harlan, *J. Leukocyte Biol.* **2005**, *77*, 129 – 140.
[6] A. M. Randi, N. I. Hogg, *J. Biol. Chem.* **1994**, *269*, 12 395 – 12 398.
[7] M. Shimaoka, T. Xiao, J.-H. Liu, Y. Yang, Y. Dong, C. D. Jun, A. McCormack, R. Zhang, A. Joachimiak, J. Takagi, J. H. Wang, T. A. Springer, *Cell* **2003**, *112*, 99 – 111.
[8] M. R. Arkin, J. A. Wells, *Nat. Rev. Drug Discovery* **2004**, *3*, 301 – 317.
[9] J. Kallen, K. Welzenbach, P. Ramage, D. Geyl, R. Kriwacki, G. Legge, S. Cottens, G. Weitz-Schmidt, U. Hommel, *J. Mol. Biol.* **1999**, *292*, 1 – 9.
[10] T. A. Kelly, D. D. Jeanfavre, D. W. McNeil, J. R. Woska, Jr., P. L. Reilly, E. A. Mainolfi, K. M. Kishimoto, G. H. Nabozny, R. Zinter, B.-J. Bormann, R. Rothlein, *J. Immunol.* **1999**, *163*, 5173 – 5177.
[11] G. Liu, J. T. Link, Z. Pei, E. B. Reilly, S. Leitza, B. Nguyen, K. C. Marsh, G. F. Okasinski, T. W. von Geldern, M. Ormes, K. Fowler, M. Gallatin, *J. Med. Chem.* **2000**, *43*, 4025 – 4040.
[12] M. Winn, E. B. Reilly, G. Liu, J. R. Huth, H.-S. Jae, J. Freeman, Z. Pei, Z. Xin, J. Lynch, J. Kester, T. W. von Geldern, S. Leitza, P. DeVries, R. Dickinson, D. Mussatto, G. F. Okasinski, *J. Med. Chem.* **2001**, *44*, 4393 – 4403.
[13] T. R. Gadek, D. J. Burdick, R. S. McDowell, M. S. Stanley, J. C. Marsters, Jr., K. J. Paris, D. A. Oare, M. E. Reynolds, C. Ladner, K. A. Zioncheck, W. P. Lee, P. Gribling, M. S. Dennis, N. J. Skelton, D. B. Tumas, K. R. Clark, S. M. Keating, M. H. Beresini, J. W. Tilley, L. G. Presta, S. C. Bodary, *Science* **2002**, *295*, 1086 – 1089.
[14] M. Shimaoka, A. Salas, W. Yang, G. Weitz-Schmitdt, T. A. Springer, *Immunity* **2003**, *19*, 391 – 402.
[15] D. J. Burdick, K. Paris, K. Weese, M. Stanley, M. Beresini, K. Clark, R. McDowell, J. C. Marsters, Jr., T. R. Gadek, *Bioorg. Med. Chem. Lett.* **2003**, *13*, 1015 – 1018.
[16] J. Bajorath, *Nat. Rev. Drug Discovery* **2002**, *1*, 882 – 894.
[17] L. Xue, J. W. Godden, J. Bajorath, *SAR QSAR Environ. Res.* **2003**, *14*, 27 – 40.
[18] P. Willett, J. M. Barnard, G. M. Downs, *J. Chem. Inf. Comput. Sci.* **1998**, *38*, 983 – 996.
[19] L. Xue, J. Bajorath, *J. Chem. Inf. Comput. Sci.* **2000**, *40*, 801 – 809.
[20] L. Xue, J. Bajorath, *J. Mol. Model.* **1999**, *5*, 97 – 102.
[21] C. A. Lipinski, F. Lombardo, B. W. Dominy, P. J. Feeney, *Adv. Drug Delivery Rev.* **1997**, *23*, 3 – 25.
[22] I. Muegge, S. L. Heald, D. Brittelli, *J. Med. Chem.* **2001**, *44*, 1841 – 1846.
[23] M. Hann, B. Hudson, X. Lewell, R. Lifely, L. Miller, N. Ramsden, *J. Chem. Inf. Comput. Sci.* **1999**, *39*, 897 – 902.
[24] Molecular Operating Environment (MOE), Chemical Computing Group Inc., Montreal, Quebec, Canada, **2005** (http://www.chemcomp.com).
[25] M. L. Dustin, O. Carpen, T. A. Springer, *J. Immunol.* **1992**, *148*, 2654 – 2663.
[26] R. Rothlein, E. A. Mainolfi, M. Czajkowski, S. D. Marlin, *J. Immunol.* **1991**, *147*, 3788 – 3793.
[27] MACCS structural keys; Elsevier MDL: San Leandro, CA, USA, **2005** (http://www.mdl.com).
[28] J. A. Hardy, J. A. Wells, *Curr. Opin. Struct. Biol.* **2004**, *14*, 706 – 715.
[29] J. Bajorath, *Curr. Drug Discov.* **2002**, *2*, 24 – 28.
[30] B. Ma, M. Shatsky, H. J. Wolfson, R. Nussinov, *Protein Sci.* **2002**, *11*, 184 – 197.
[31] J. Boström, A. Hogner, *J. Med. Chem.* **2006**, *49*, 6716 – 6725.
[32] R. Nilakantan, F. Immermann, K. A. Haraki, *Comb. Chem. High Throughput Screening* **2002**, *5*, 105 – 110.

Received: December 9, 2006
Published online on March 6, 2007

